Clim Dyn (2017) 48:987–997
DOI 10.1007/s00382-016-3123-6

Relative roles of differential SST warming, uniform SST warming and land surface warming in determining the Walker circulation changes under global warming

Lei Zhang[1] · **Tim Li**[1,2]

Received: 8 December 2015 / Accepted: 3 April 2016 / Published online: 18 April 2016

Abstract Most of CMIP5 models projected a weakened Walker circulation in tropical Pacific, but what causes such change is still an open question. By conducting idealized numerical simulations separating the effects of the spatially uniform sea surface temperature (SST) warming, extra land surface warming and differential SST warming, we demonstrate that the weakening of the Walker circulation is attributed to the western North Pacific (WNP) monsoon and South America land effects. The effect of the uniform SST warming is through so-called "richest-get-richer" mechanism. In response to a uniform surface warming, the WNP monsoon is enhanced by competing moisture with other large-scale convective branches. The strengthened WNP monsoon further induces surface westerlies in the equatorial western-central Pacific, weakening the Walker circulation. The increase of the greenhouse gases leads to a larger land surface warming than ocean surface. As a result, a greater thermal contrast occurs between American Continent and equatorial Pacific. The so-induced zonal pressure gradient anomaly forces low-level westerly anomalies over the equatorial eastern Pacific and weakens the Walker circulation. The differential SST warming also plays a role in driving low-level westerly anomalies over tropical Pacific. But such an effect involves a positive air-sea feedback that amplifies the weakening of both east–west SST gradient and Pacific trade winds.

Keywords Global warming · The Walker circulation · Uniform SST warming and extra land warming

✉ Tim Li
timli@hawaii.edu

Lei Zhang
zhanglei@hawaii.edu

[1] IPRC and Department of Atmospheric Sciences, University of Hawaii, 2525 Correa Rd., Honolulu, HI 96822, USA

[2] International Laboratory on Climate and Environment Change and Key Laboratory of Meteorological Disaster of Ministry of Education, Nanjing University of Information Science and Technology, Nanjing, China

1 Introduction

The earth is warming due to the emission of greenhouse gases (GHGs) associated with anthropogenic activities since industrial revolution, with an increasing rate of global mean surface temperature around 0.1–0.15 K decade^{-1} based on the intergovernmental panel on climate change (IPCC) Fourth Assessment report (AR4) (IPCC 2007). Given the pronounced warming rate, the impacts of global warming draw lots of attention and have been studied intensively (Manabe et al. 1990, 1991; Vecchi and Soden 2007; Knutson et al. 2010; Li et al. 2010; Xie et al. 2010; Murakami et al. 2011, 2012; Zhao and Held 2010, 2012).

Tropical precipitation provides large amount of energy for the global climate system, and the changes of coupled atmosphere–ocean system in the tropics under global warming have been widely examined (e.g. Vecchi et al. 2008; Xie et al. 2010; Hsu and Li 2012; Zhang 2016). In particular, since it has been shown that the anomalous Walker circulation influences weather and climate systems globally (Hoskins and Karoly 1981; Wallace and gutzler 1981; Wang et al. 2000), the responses of the Walker circulation to global warming has been analyzed intensively (Knutson and Manabe 1995; Clement et al. 1996; Cane et al. 1997; Vecchi et al. 2006; Held and Soden 2006; Vecchi and Soden 2007; DiNezio et al. 2009; Collins et al. 2010; DiNezio et al. 2010; Schneider et al. 2010). Some studies have suggested that the Walker circulation has been

strengthening in the past (Sandeep et al. 2014), whereas Vecchi et al. (2006) found that the zonal sea level pressure (SLP) gradient in tropical Pacific has been weakening due to anthropogenic forcing. In contrast, the future projections from most climate models that participate in coupled model inter-comparison project phase 5 (CMIP5) predominantly simulate a weakened Walker circulation under global warming (Fig. 1a). Since this is the region where air-sea coupling is extraordinarily active (Bjerknes 1969), it is not surprising that CMIP5 multi-model mean results show a weaker east–west sea surface temperature (SST) gradient in the equatorial Pacific as well (Fig. 1a). Figure 1b shows that the major rainfall center in the warm pool region shifts eastward and anomalous subsidence occupies the Maritime Continent region, which are also consistent with weakened Walker circulation.

In tropical Pacific, the weakened Walker circulation and the El Nino like SST warming are closely related through air-sea interactions. What are the causes of the formation of a weakened Walker circulation/El Nino like SST warming? It is noted that the positive atmosphere–ocean feedback, i.e., the Bjerknes feedback, can favor either an El Nino like SST warming or a La Nina like cooling, depending on the sign of the initial perturbation, and therefore, such process is an amplifier. In contrast, Zhang and Li (2014) found that the formation of the El Nino like SST warming essentially arises from a "longwave radiative—evaporative damping" mechanism: in western (eastern) tropical Pacific, where the mean-state surface latent heat flux and SST are relatively large (small), it requires a smaller (greater) ocean warming response to cancel out the imposed longwave radiative forcing. The weakened east–west SST gradient is further amplified through cloud feedback associated with the weakened Walker circulation (Zhang and Li 2014). In addition to this mean state-determined SST gradient changes, are there other causes of the weakening of the Walker circulation under global warming? Knutson and Manabe (1995) analyzed increased CO_2 concentration-induced changes in their coupled climate model, and they found that the static stability in the troposphere became greater due to GHG effect, which may result in the weakening of atmospheric circulation. Held and Soden (2006) examined the future projections from climate models and found that the global mean precipitation increases at a much slower rate (1–2 % per degree surface warming) than moisture (6–7 %, Clausius-Clapeyron equation). This result suggests that the global mean upward mass flux is reduced and therefore atmospheric overturning circulation is weakened under global warming. However, by analyzing a uniform SST warming experiment with an aqua-planet setting, Li et al. (2015) found that the Walker circulation is strengthened in a warmer climate, with similar rainfall-moisture "mismatch"

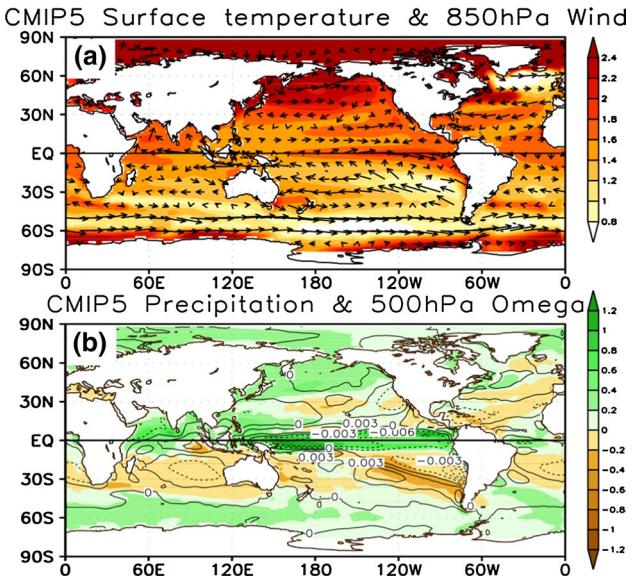

Fig. 1 **a** Multi-model mean differences of annual mean surface temperature (shading, K) and 850 hPa winds (vector, m s^{-1}) between present day (1986–2005) and global warming (2081–2100) climate states from CMIP5 climate models. **b** Same as (**a**) but for precipitation (*shading*, mm day^{-1}) and 500 hPa omega changes (contour, Pa s^{-1})

and enhanced tropospheric static stability. Such a result indicates that the aforementioned mechanisms may not be sufficient to explain the weakened Walker circulation in a warmer climate. This result also implies that the presence of the continents may play an essential role in the projected weakening of the Walker circulation.

Given the great impacts of the Walker circulation changes on global climate system, we aim to reveal the causes of the weakening of the Walker circulation by analyzing outputs from CMIP5 climate models and conducting numerical experiments.

2 Model and methodology

To explore the causes of the projected weakening of the Walker circulation in addition to the El Nino like SST warming, a uniform SST warming experiment was conducted using atmospheric general circulation model (AGCM) ECHAM4.6 (Roeckner et al. 1996) at T42 horizontal resolution. In addition to the control run (CTRL), which was forced by the monthly climatological SST field, 2 K uniform SST warming was added globally in the sensitivity experiment. In both experiments, model was integrated for 20 years and results from the last 15 years were analyzed.

As demonstrated in the following sections, it is hypothesized that the uniform warming and extra land warming

Table 1 Fifteen CMIP5 climate models analyzed in this study

Model	Modeling center (Group)	AGCM resolution
ACCESS1-0	The Centre for Australian Weather and Climate Research	1.875° × 1.25°
BCC-CSM1.1	Beijing Climate Center, China Meteorological Administration	2.8125° × 2.8125°
CanESM2	Canadian Centre for Climate Modelling and Analysis	2.8125° × 2.8125°
CNRM-CM5	Centre National de Recherches Meteorologiques/Centre Europeen de Recherche et Formation Avancees en Calcul Scientifique	1.40625° × 1.40625°
GFDL-CM3	Geophysical Fluid Dynamics Laboratory	2.5° × 2°
GFDL-ESM2 M	NOAA GFDL	2.5° × 2°
GISS-E2-R	NASA Goddard Institute for Space Studies	2.5° × 2°
HadGEM2-CC	Met Office Hadley Centre	1.875° × 1.24°
HadGEM2-ES		
IPSL-CM5A-LR	Institut Pierre-Simon Laplace	3.75° × 1.875°
IPSL-CM5A-MR		2.5° × 1.258°
MIROC-ESM	Japan Agency for Marine-Earth Science and Technology, Atmosphere and Ocean Research Institute (The University of Tokyo), and National Institute for Environmental Studies	2.8125° × 2.8125°
MIROC-ESM-CHEM		
MPI-ESM-LR	Max Planck Institute for Meteorology	1.875° × 1.875°
NorESM1-M	Norwegian Climate Centre	2.5° × 1.875°

Monthly horizontal winds, surface temperature, vertical motion and precipitation are analyzed

may cause weakening of the Pacific trade winds, and hence, the responses of the Walker circulation to different surface warming were explored, using idealized numerical experiments. To obtain the differential SST warming pattern and to determine the magnitudes of mean SST warming and additional land surface warming, monthly outputs from CMIP5 climate models were analyzed. Fifteen climate models were available for analysis (Table 1), and both historical runs and future projections under representative concentration pathway 4.5 (RCP4.5) from these models were analyzed. In RCP4.5, the radiative forcing reaches 4.5 W/m^2 (equivalent to 650 ppm CO_2 concentration) in 2100 and stabilizes after that. The changes in a warmer climate are defined as the differences between present-day (1986–2005) and global-warming (2081–2100) climate states.

It is noted that the projected land surface warming is evidently greater than the ocean, which is hypothesized to play an important role in the weakening of the Walker circulation (Fig. 2a, b). The effects of SST warming and land surface warming were thereby explored separately through idealized numerical simulations, in which the land surface temperatures were prescribed (diurnal cycle included). This is in contrast to the AGCM experiment with an interactive land surface, such as the 2 K uniform SST warming experiment described above. The differences of the mean states between prescribed and interactive land surface experiments are examined (Fig. 3). Overall, the mean states are similar between the two experiments, but it is noted that the land rainfall is greater in Fig. 3b. This is because precipitation tend to cool the land surface, but such an interactive

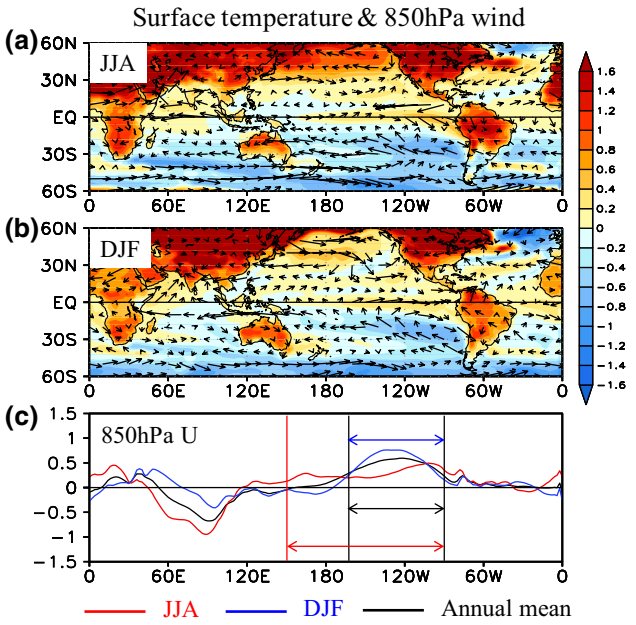

Fig. 2 Multi-model mean differences of surface temperature (unit: K; tropical annual mean SST warming between 30°S and 30°N is removed) and 850 hPa winds (vector, m s^{-1}) between 2081–2100 and 1986–2005 in **a** JJA and **b** DJF, respectively. **c** 850 hPa zonal wind changes averaged between 5°S and 5°N (units, m s^{-1}) in boreal summer (*red*) and winter (*blue*), and *black* for annual mean changes. *Arrows* denote regions with significant westerly anomalies in different seasons

process is precluded when the land surface temperature is prescribed. To exclude the impacts of different mean states due to the prescribed land surface temperature, land surface

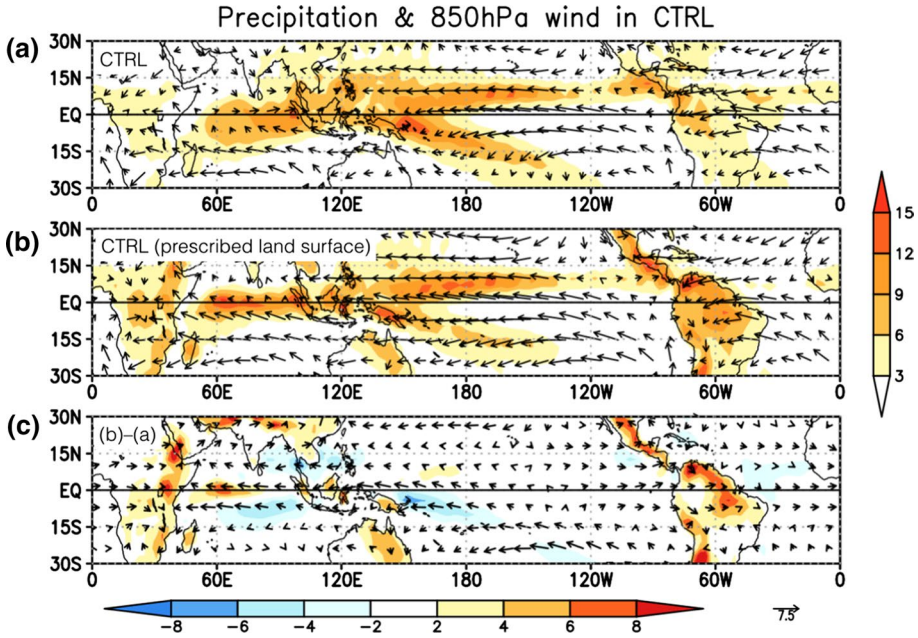

Fig. 3 **a** Climatological annual mean precipitation field (mm day^{-1}) and 850 hPa winds (m s^{-1}) in control run using ECHAM4.6 with an interactive land surface. **b** Same as (**a**) but for the numerical experiment with land surface temperatures being prescribed to the same climatological values as in (**a**). **c** The differences between (**a**) and (**b**)

temperatures are prescribed in both CTRL and sensitivity experiments. However, a caution is needed, as the present-day biases may affect the climate change processes in the climate models.

In addition to CTRL, which is forced by climatological surface temperature fields over both land and ocean, four sensitivity experiments were carried out: (1) monthly differential SST warming (tropical annual mean SST warming removed) from CMIP5 models was added to the climatological SST field, while land surface temperatures remain the same as in CTRL; (2) 1.5 K uniform warming, which is the tropical annual mean SST warming derived from CMIP5 models, was added to both ocean and land surfaces compared to CTRL; (3) 0.9 K warming is added to the land surface, while SST field has no difference from CTRL. The value 0.9 K is the average excessive land surface warming compared to the ocean surface in the tropical region in CMIP5 models; (4) monthly surface warming from CMIP5 climate models (differential SST warming, uniform surface warming and excessive land surface warming pattern all included) is added to the climatological surface temperature field used in CTRL. For each experiment, the model was integrated for 30 years and last 20 years were analyzed. By comparing the first three sensitivity experiments with CTRL, the effects of differential SST warming, uniform surface warming and land-sea warming contrast on Walker circulation changes were analyzed. Differences between experiment (4) and CTRL are compared to the projected rainfall changes in CMIP5 models to validate the performance of our numerical simulations.

3 Weakening of the Walker circulation

Aside from a nearly ubiquitous surface warming, a pronounced differential warming pattern shows up in the future projections from CMIP5 models (Fig. 2). Warming in the land area is greater than the ocean and an El Nino like SST warming shows up in tropical Pacific. There is an inter-hemispheric contrast in Pacific SST warming (greater warming in northern hemisphere), which is relatively more evident in boreal summer (June, July, August, JJA) (Fig. 2a, b). It is noted that the low-level westerly anomalies occupy the entire equatorial Pacific in JJA, whereas the relaxed trade winds are mainly located over equatorial central-eastern Pacific in boreal winter (December, January, February, DJF) (Fig. 2c). Annual mean Pacific trade wind changes are similar to the winter season (Fig. 2c). It is thus clear that the Walker circulation is projected to be weakened in both seasons, and the causes of such changes are explored in the following sections.

3.1 Hypotheses for the projected weakening of the Walker circulation

The east–west SST gradient in tropical pacific is projected to be weakened (Fig. 2), which may play a role in driving low-level westerly anomalies. But such an effect involves a positive air-sea feedback that amplifies the weakening of both east–west SST gradient and Pacific trade winds. To explore the fundamental cause of the projected weakening of the Walker circulation, a uniform SST warming experiment that precludes the impacts of SST gradients changes

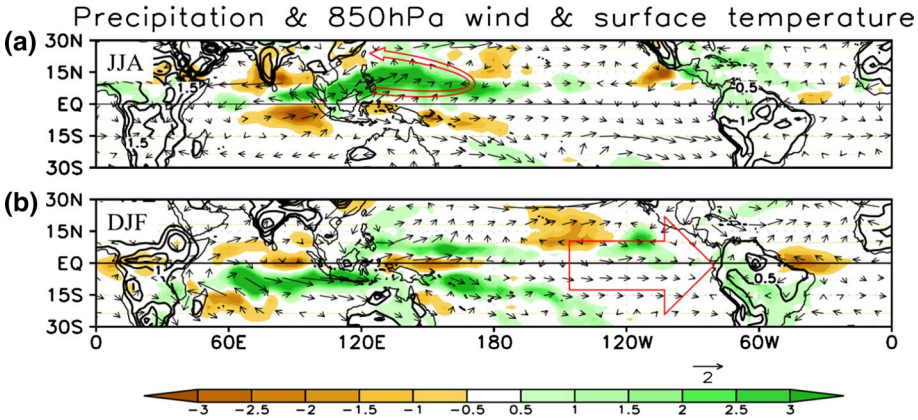

Fig. 4 Differences of 850 hPa winds (vector, m s^{-1}) and precipitation (shading, mm day^{-1}) between a 2 K uniform SST warming experiment and CTRL in **a** JJA and **b** DJF. *Contours* represent land surface temperature changes with 2 K uniform warming removed (contour, K). *Red arrows* denote **a** low-level cyclonic wind anomaly over WNP region and **b** low-level westerly anomalies over eastern Pacific

was conducted. Given the pronounced seasonality in projected trade wind changes in CMIP5 models (Fig. 2c), the uniform SST warming-induced changes in boreal summer and winter are analyzed separately. It is noted that the low-level westerly anomalies show up over equatorial Pacific in both seasons, which suggests that the Walker circulation is weakened even when the ocean surface is uniformly warmed.

The low-level westerly anomalies are mainly located over equatorial western Pacific in boreal summer, which seems related to the anomalous low-level cyclonic gyre associated with positive precipitation anomaly in western North Pacific (WNP) region (Fig. 4a). Such a result is consistent with the so-called "richest-get-richer" mechanism: greater water vapor availability in a warmer climate leads to a greater moisture convergence that enhances WNP rainfall; the enhanced precipitation/heating in turn forces anomalous large-scale convergent flow that further intensifies the positive rainfall anomalies in WNP region, whereas the adjacent relatively weaker rainfall centers are suppressed due to the circulation changes. It is then hypothesized that the WNP monsoon trough is enhanced by competing moisture with other adjacent convective branches under the influence of uniform warming, and this process eventually leads to low-level cyclonic wind anomalies over WNP and associated westerly anomalies over equatorial western Pacific, weakening the Walker circulation.

Another robust feature found in both uniform SST warming experiment and future projections from CMIP5 models is the greater surface warming over land than the ocean. Such land-sea warming contrast is due to small surface latent heat flux over land climatologically, which leads to the GHG effect-induced surface longwave radiation increase being primarily balanced by greater surface sensible heat release through raising land surface temperature. The additional land warming leads to lower SLP over American Continent compared to the adjacent eastern Pacific (EP) region (figure not shown). Hence, it is hypothesized that changes in zonal SLP gradients may force low-level westerly anomalies over tropical EP that weakens the Walker circulation (Fig. 4). A recent study by Bayr et al. (2014) also pointed out the importance of greater land warming on the projected Walker circulation changes.

3.2 Uniform warming and additional land warming effects

Given the aforementioned hypotheses, idealized numerical simulations that separate the effects of different surface warming patterns are analyzed here to explore the relative roles of uniform warming (through "richest-get-richer" mechanism) and excessive land surface warming (through inducing SLP gradients changes) in causing the projected Walker circulation changes under global warming. Differential SST warming effect is also examined for comparison, but it was pointed out by Zhang and Li (2014) that the formation of the El Nino like SST warming in the climate models is partly attributed to the weakened Walker circulation, and therefore, the differential SST warming effect involves air-sea positive feedback that serves as an amplifier.

3.2.1 Weakened trade winds in boreal summer and winter

Atmospheric responses to different surface warming patterns in different seasons are analyzed firstly. Changes of low-level winds and precipitation in boreal summer are shown in Fig. 5. An El-Nino like SST warming, enhanced equatorial warming and an evident inter-hemispheric warming contrast show up in JJA (Fig. 5a). Correspondingly, major rainfall center shifts eastward and low-level trade winds are weakened in equatorial Pacific, and prominent anomalous southerly cross-equatorial flows appear over tropical Pacific. Over WNP, an anomalous low-level anti-cyclone and negative rainfall anomalies occupy Philippine Sea in response to the differential SST warming (Fig. 5a). Previous studies suggest that rainfall changes in WNP is dynamically linked to the Indian summer monsoon

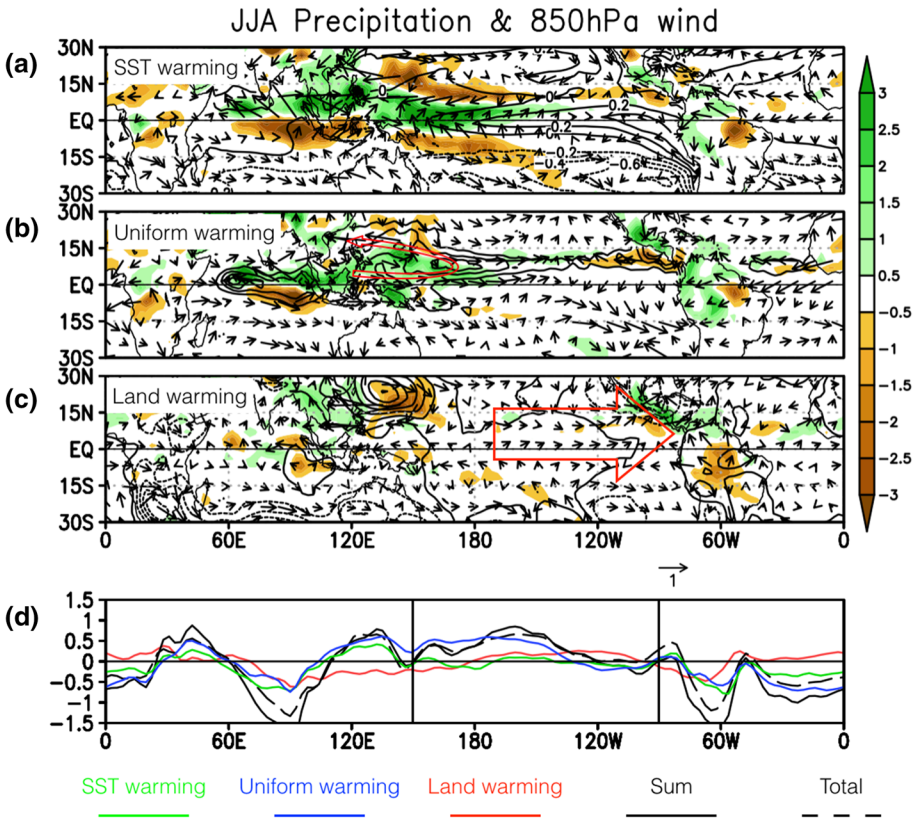

Fig. 5 **a** Changes of precipitation (shading, mm day^{-1}) and 850 hPa winds (vector, m s^{-1}) in JJA due to differential SST warming effect, contours denote differential SST warming pattern with tropical mean SST warming removed (0.2 K interval); **b** Same as (**a**), but for changes due to the uniform surface warming effect, and contours denote precipitation distribution in the ocean in CTRL (5 mm day^{-1} interval); **c** Changes due to excessive land warming, and contours denote SLP changes (solid for positive SLP anomalies and dashed for negative SLP anomalies with a 0.2 hPa interval). **d** 850 hPa zonal wind changes (averaged between 5°S and 5°N) due to the effects of differential SST warming (*green*), uniform warming (*blue*) and excessive land warming (*red*), and *solid black line* is the sum of the three curves. *Dashed black curve* is for zonal wind changes due to the total surface warming (experiment (4) minus CTRL). Units are m s^{-1}. *Red arrows* denote **b** low-level cyclonic wind anomaly over WNP region and **c** low-level westerly anomalies over eastern Pacific. *Black lines* in **d** denote the region with significant westerly anomalies (same as Fig. 2c)

(ISM) rainfall anomaly, with an out-of-phase relationship (Chang and Li 2000; Wang et al. 2013). Hence, the weakened WNPSM rainfall may be related to the enhanced ISM associated with the SST anomaly dipole in Indian Ocean (IO).

The uniform warming-induced changes in JJA are shown in Fig. 5b. Climatologically, major rainfall centers are primarily located at northern hemisphere in boreal summer, i.e. WNPSM and ISM (Fig. 5b). In response to the uniform warming, with no changes in land-sea thermal contrast or SST gradients, positive precipitation anomaly as well as low-level anomalous cyclonic flow appear in WNP region (Fig. 5b), suggesting that the WNP monsoon trough is enhanced. Such a result is consistent with the "richest-get-richer" theory. Consequently, low-level westerly anomalies show up over equatorial central-western Pacific (Fig. 5b). Figure 5c shows the changes due to additional land warming effect in boreal summer. Rainfall in North America and Southeast Asia is enhanced due to higher surface temperature. Positive precipitation anomalies and warmer land surface lead to lower SLP over North America, which alters the zonal SLP gradient and thereby forces large-scale low-level westerly anomalies over tropical EP region (Fig. 5c).

The atmospheric responses to surface warming in boreal winter are shown in Fig. 6. With an El Nino-like SST warming in tropical Pacific, precipitation is enhanced in equatorial central Pacific and low-level westerly anomalies occur over equatorial central-eastern Pacific, weakening the trade winds (Fig. 6a). Compared to JJA, the anomalous southerly cross-equatorial flow over equatorial Pacific are less evident, which agrees with smaller inter-hemispheric warming contrast in DJF (Fig. 2). In contrast, the uniform surface warming-induced positive precipitation anomalies are mainly located at western Pacific warm pool region and south Pacific convergence zone (SPCZ), following the climatological precipitation distribution in DJF (Fig. 6b).

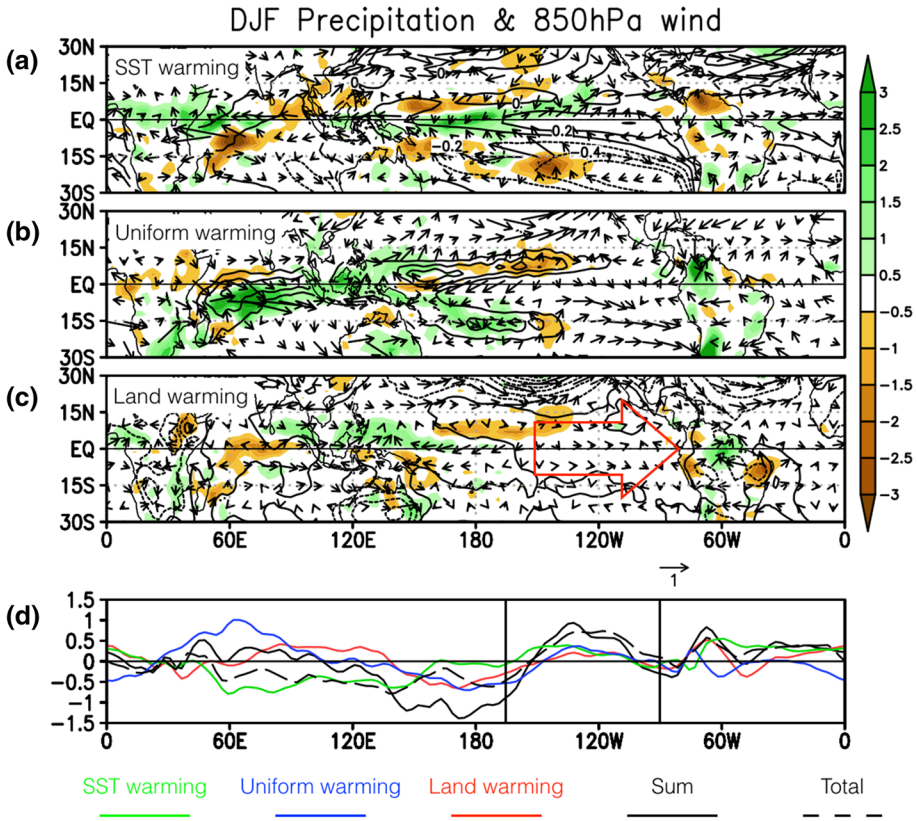

Fig. 6 Same as Fig. 5, but for changes in boreal winter (DJF). *Red arrow* in **c** denotes low-level westerly anomalies over eastern Pacific region

Rainfall also increases in South America, which induces anomalous large-scale low-level westerlies over subtropical EP in southern hemisphere (Fig. 6b). In IO, climatological rainfall center shifts southward in DJF, and correspondingly, positive precipitation anomalies are located to the south of equator, with prominent northerly anomalies over equatorial IO (Fig. 6b). Due to the excessive land warming, low-level westerly anomalies show up over equatorial EP (Fig. 6c), which is associated with changes in zonal SLP gradients in the EP-American Continent sector due to lower SLP over South America (Fig. 6c). Anomalous large-scale flows toward Australia also occur over south IO in response to the additional land warming (Fig. 6c).

To sum up, the uniform warming and additional land warming effects indeed contribute to the weakened Walker circulation. While the former effect leads to westerly anomalies over equatorial central-western Pacific in JJA, changes in land-sea thermal contrast is responsible for the occurrence of low-level westerly anomalies over equatorial EP in both boreal summer and winter (Figs. 5d, 6d). Differential SST warming also contributes to the weakened trade winds. It is noted that the total westerly anomalies occupy the entire equatorial Pacific in JJA (Fig. 5d), whereas the westerly anomalies are mainly located over equatorial EP region in DJF (Fig. 6d). These results are in agreement with projections from CMIP5 models (Fig. 2c). It is interesting to note that over equatorial western Pacific, the excessive land warming effect generates low-level easterly anomalies that enhance Pacific trade wind, which might be associated with additional warming in Maritime Continent (Figs. 5, 6).

3.2.2 *Annual mean trade wind changes*

The annual mean changes of precipitation and low-level winds due to different surface warming effects are analyzed (Fig. 7). The annual mean differential SST warming still exhibits an El Nino-like warming and an enhanced equatorial warming in tropical Pacific (Fig. 7a). Correspondingly, major rainfall center displaces eastward in the equatorial central Pacific, and the subtropical region becomes drier. Low-level westerly anomalies show up in equatorial central-eastern Pacific, which agrees with warmer SST in EP. Anomalous southerly cross-equatorial flows emerge over the equatorial Pacific in response to the inter-hemispheric warming contrast. In IO, the SST warming dipole induces low-level southeasterly anomalies in the equatorial region and a precipitation change dipole.

In contrast to the differential SST warming-induced changes, the annual mean positive rainfall anomalies due to the uniform warming effect generally follow the "richest" climatological precipitation centers in the tropics, i.e. IO-western Pacific warm pool region (Fig. 7b). In tropical Pacific, the enhanced rainfall in WNP region is associated with a low-level cyclonic gyre anomaly, which leads to

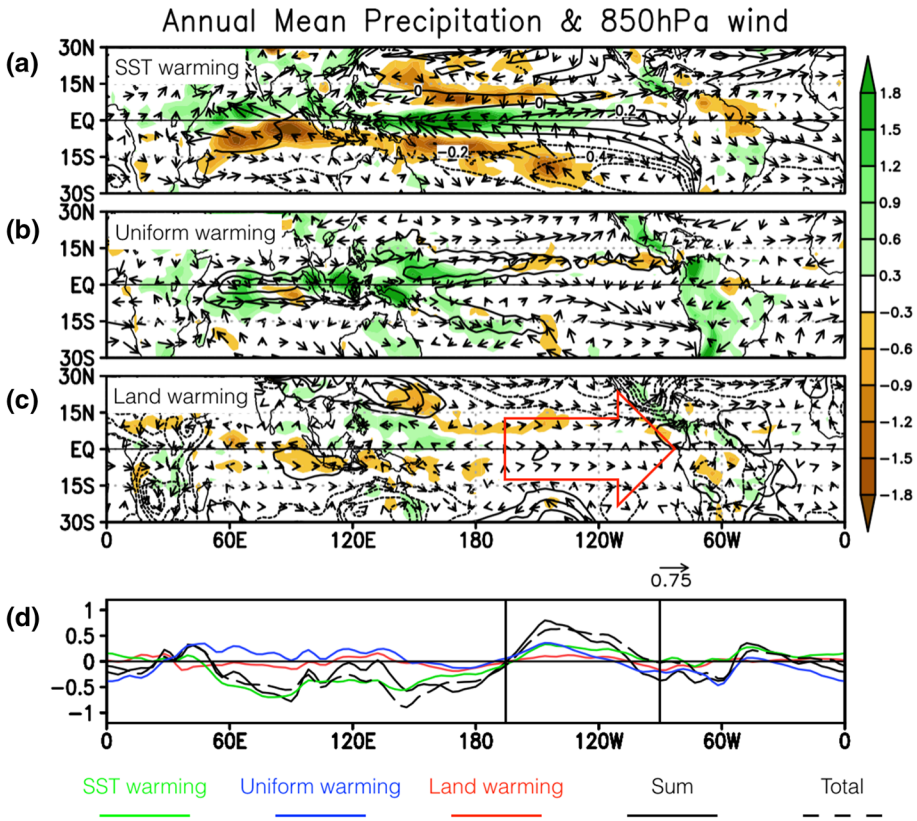

Fig. 7 Same as Fig. 5, but for annual mean changes. The contour interval in (**c**) is 0.1 hPa. *Red arrow* in **c** denotes low-level westerly anomalies over eastern Pacific region

westerly anomalies in Maritime Continent region (Fig. 7b). Over subtropical region, large-scale westerly anomalies toward American Continent show up in both northern and southern subtropical Pacific, which are associated with enhanced land rainfall. The excessive land warming-induced changes are shown in Fig. 7c. Overall, the anomalous low-level winds are directed toward the continental region where SLP anomalies are negative. It is noted that the trade winds are enhanced over equatorial western Pacific, which might be associated with additional warming in Maritime Continent. More importantly, warmer land surface over American Continent leads to lower SLP in situ and forces low-level westerly anomalies over equatorial EP through changes in zonal SLP gradients (Fig. 7c). Annual mean westerly anomalies induced by the surface warming effects are mainly located at equatorial central-eastern Pacific (Fig. 7d), which is consistent with the annual mean Pacific trade wind changes in CMIP5 models (Fig. 2c).

It is noted that the zonal wind changes due to the total surface warming agree with the sum of zonal wind changes induced by different surface warming effects reasonably well, albeit some discrepancies in the IO-western Pacific sector in DJF (Figs. 5d, 6d, 7d). This suggests that the total warming effect on Walker circulation changes is reasonably separated through idealized numerical experiments. The area averaged zonal wind changes over equatorial central-eastern Pacific were calculated, and it is found that

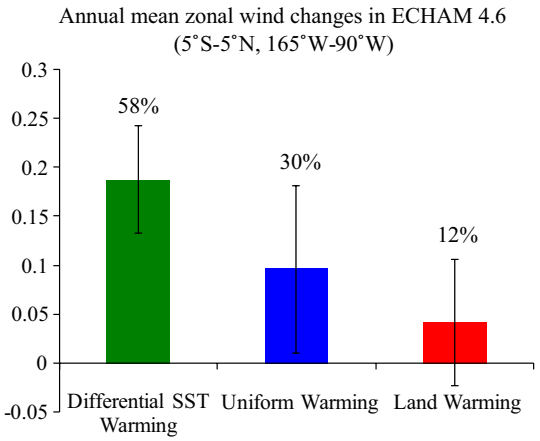

Fig. 8 Area averaged (5°S–5°N, 165°W–90°W) annual mean 850 hPa zonal wind changes due to the effects of differential SST warming (*green*), uniform warming (*blue*) and additional land warming (*red*). Units are m s^{-1}. *Vertical error bars* denote the SD. Numbers above the *bars* are the percentages of zonal wind changes due to the three factors

the weakening of the Pacific trade wind is mostly attributed to the differential SST warming effect, which contributes to around 58 % of total zonal wind changes (Fig. 8). Uniform warming and extra land warming effects lead to 30 and 12 % weakening of the trade winds, respectively. Although differential SST warming plays an important role

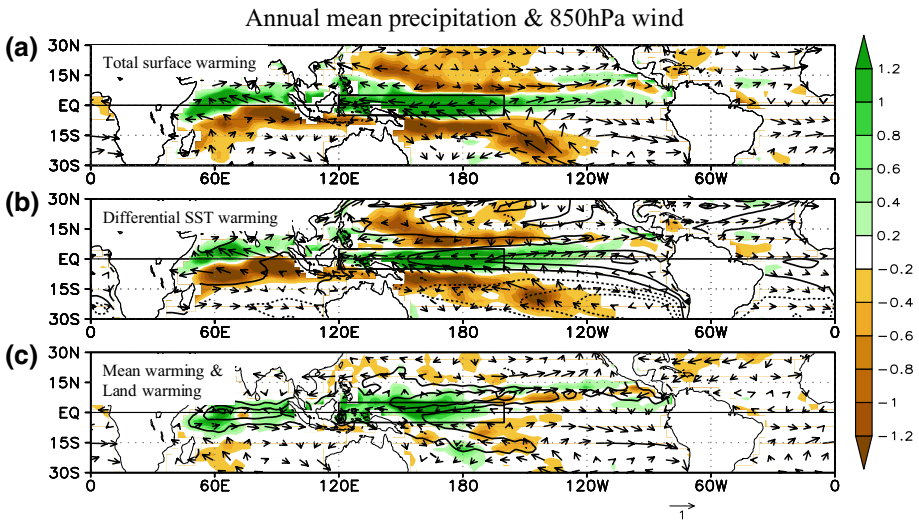

Fig. 9 Annual mean changes of precipitation (units: mm day^{-1}) and 850 hPa winds (units: m s^{-1}) due to **a** total surface warming effect and **b** differential SST warming effect. **c** The differences between (**a**) and (**b**), which are due to the effects of both uniform warming and land warming. *Contours* represent **b** differential SST warming (K, 0.2 K interval) and **c** rainfall field in CTRL (mm day^{-1}, 5 mm day^{-1} interval). *Box* denotes the region with evident positive rainfall anomalies over tropical Pacific in (**a**) (5°S–5°N, 120°E–160°W)

in driving low-level zonal wind changes over equatorial Pacific, this effect already involves a positive air-sea feedback process. In contrast, both uniform warming (through "richest-get-richer" mechanism) and additional land warming effects are independent of SST gradients changes, and therefore, they are fundamental causes of the weakening of the Walker circulation in a warmer climate.

4 Relative roles of different surface warming patterns in determining precipitation changes

In addition to the changes in Pacific trade winds, the relative roles of different surface warming patterns in determining precipitation changes are also explored. The total surface warming-induced changes are shown in Fig. 9a. Overall, the projected precipitation changes in CMIP5 models are reproduced reasonably well, including the precipitation anomaly dipole in IO and the enhanced rainfall in equatorial Pacific (Figs. 1b, 9a). Although it is noted that there are substantial discrepancies in the zonal wind changes over equatorial western Pacific between Figs. 1a and 9a.

Figure 9b shows the atmospheric responses to the differential SST warming. Positive (negative) rainfall anomalies show up in tropical (subtropical) Pacific due to enhanced equatorial warming. The rainfall anomaly dipole in IO also agrees with greater warming in north IO (Fig. 9b). These results are consistent with the so-called "warmer-get-wetter" theory (Xie et al. 2010), which predicts more (less) rainfall in the tropical region where SST warming is greater (smaller) than the tropical mean SST warming. The differences between Fig. 9a and b are shown in Fig. 9c, which are attributed to the effects of both uniform warming and additional land warming. It is found that the positive precipitation anomalies follow the major climatological rainfall centers, i.e. IO-western Pacific warm pool region (Fig. 9c).

The remarkable similarities between Fig. 9a and b suggest that a large portion of the projected annual mean precipitation changes in climate models is attributed to the differential SST warming effect. But other forcing also plays a role, especially in the enhanced rainfall in equatorial IO and equatorial central-western Pacific (Fig. 9c). The unequal SST warming effect accounts for 63 % of total rainfall changes in equatorial central-western Pacific, where most significant positive precipitation anomalies are located at, and other forcing contributes to 37 % of total changes. This result is consistent with the finding in the previous section that almost 60 % of westerly anomalies over equatorial central-eastern Pacific are due to the differential SST warming effect (Fig. 8), but it is worth stressing that the formation of such differential SST warming has already involved the air-sea interaction process.

5 Discussion and conclusions

Most of CMIP5 climate models projected a weakened Walker circulation and an El Nino like SST warming in tropical Pacific due to the GHG effect. It is further noted that trade winds over tropical Pacific are weakened even in a uniform SST warming experiment, with no changes in SST gradients. By conducting numerical experiments that separate the effects of uniform warming, additional land warming and differential SST warming, the fundamental cause of the projected weakening of the Walker circulation in a warmer climate is investigated.

Our numerical simulations demonstrate that the uniform warming and excessive land warming can weaken the

Walker circulation. They can cause 30 and 12 % weakening of the annual mean trade winds over equatorial central-eastern Pacific, respectively. In response to a uniform warming, the WNPSM is enhanced in JJA, accompanied by a low-level cyclonic circulation anomaly, which is consistent with the "richest-get-richer" theory. Consequently, the uniform warming-induced surface westerly anomalies show up over equatorial western-central Pacific in boreal summer, leading to the weakening of the Walker circulation. The extra land surface warming, which is a robust feature in the future projections from all climate models, leads to a greater land–ocean thermal contrast, which changes zonal SLP gradients and drives anomalous low-level westerlies over EP-American Continent sector.

The differential SST warming contributes to 58 % weakening of the annual mean low-level zonal winds over the equatorial central-eastern Pacific. However, this process has already involved a positive air-sea feedback process that amplifies weakening of both east–west SST gradient and Pacific trade winds. In contrast, both the uniform SST warming ("richest-get-richer") and additional land warming effects are independent of SST gradients changes, and therefore, they are the fundamental causes of the weakened Walker circulation over the equatorial Pacific. These two mechanisms are complimentary to a previously identified "longwave radiative—evaporative damping" mechanism suggested by Zhang and Li (2014), which explains the formation of the El Nino like SST warming even with no atmospheric feedback involved. It is also worth mentioning that the WNPSM and land warming effects are both related to the presence and positions of the continents, which were precluded in the aqua-planet simulation with which Li et al. (2015) found a strengthened Walker circulation.

Finally, the effects of the three factors on precipitation changes are also examined. It is found that the differential SST warming effect explains a large portion (63 %) of the rainfall changes in tropical Pacific under global warming. This result is consistent with the "warmer-get-wetter" mechanism. The uniform warming and the extra land warming also contribute significantly to the projected rainfall changes in tropical Pacific (37 %).

It is noted that some observational studies have found strengthening of the Walker circulation and an evident EP cooling anomaly in recent decades (Trenberth et al. 2014; England et al. 2014; Zhang 2016). However, based on the analysis in this study, the EP cooling would lead to an enhanced land–ocean thermal contrast, which is supposed to weaken the Pacific trade wind. It should be noted that these two results, i.e., the enhanced land–ocean thermal contrast and intensification of the Walker circulation, are not necessarily in conflict with each other because in addition to the prominent EP cooling, there are other SST anomaly patterns that are important for the Walker circulation changes. For instance, the enhanced east–west SST gradient in the tropical Pacific associated with inter-decadal Pacific oscillation (Trenberth et al. 2014), the greater warming in Indian Ocean (Luo et al. 2012) and Atlantic (McGregor et al. 2014) compared to the tropical Pacific, have been suggested to contribute to the intensification of the Walker circulation. These mechanisms might be responsible for the observed strengthening of the Walker circulation in recent decades, despite the greater land–ocean thermal contrast.

One limitation of this study is that only one AGCM was used to conduct the idealized numerical simulations, while there are substantial intermodel discrepancies in the projected future rainfall changes, which may affect the changes of the Walker circulation. Besides, the long-term change of the Walker circulation in observation is still unclear. Therefore, idealized numerical experiments using different models and more observational studies are still needed for better understanding of the changes of the Walker circulation under global warming.

Acknowledgments This work was supported by China National 973 project 2015CB453200, NRL grant N00173-13-1-G902, ONR grant N00014-16-12260 and the International Pacific Research Center that is sponsored by the Japan Agency for Marine-Earth Science and Technology (JAMSTEC). All the datasets from CMIP5 models can be accessed through ESGF data portals (http://pcmdi-cmip.llnl.gov/cmip5/availability.html). This is SOEST contribution number 9611, IPRC contribution number 1185, and ESMC contribution number 101.

References

Bayr T, Dommenget D, Martin T, Power SB (2014) The eastward shift of the Walker circulation in response to global warming and its relationship to ENSO variability. Dyn Clim. doi:10.1007/s00382-014-2091-y

Bjerknes J (1969) Atmospheric teleconnections from the equatorial Pacific. Mon Wea Rev 97:163–172

Cane MA, Clement AC, Kaplan A, Kushnir Y, Pozdnyakov D, Seager R, Zebiak SE, Murtugudde R (1997) Twentieth-century sea surface temperature trends. Science 275:957–960

Chang CP, Li T (2000) A theory for the tropical tropospheric biennial oscillation. J Atmos Sci 57(14):2209–2224

Clement AC, Seager R, Cane MA, Zebiak SE (1996) An ocean dynamical. Thermostat J Clim 9:2190–2196

Collins M et al (2010) The impact of global warming on the tropical Pacific Ocean and El Nino. Nature Geosci 3:391–397

DiNezio P, Clement A, Vecchi GA, Soden B, Kirtman BP (2009) Climate response of the Equatorial Pacific to global warming. J Clim 22:4873–4892

DiNezio P, Clement A, Vecchi GA (2010) Reconciling differing views of tropical pacific climate change. EOS. 91(16):141–152

England MH, McGregor S, Spence P et al (2014) Recent intensification of wind-driven circulation in the Pacific and the ongoing warming hiatus. Nat Climate Change 4:222–227

Held IM, Soden BJ (2006) Robust responses of the hydrological cycle to global warming. J Clim 19:5686–5699

Hoskins BJ, Karoly DJ (1981) The steady linear response of a spherical atmosphere to thermal and orographic forcing. J Atmos Sci 38(6):1179–1196

Hsu P-C, Li T (2012) Is "rich-get-richer" valid for Indian ocean and Atlantic ITCZ? Geophys Res Lett 39:L13705. doi:10.1029/2012GL052399

IPCC (2007) Climate change 2007: the physical science basis. In: Solomon S et al (eds) Contribution of working group I to the fourth assessment report of the intergovernmental panel on climate change. Cambridge University Press, Cambridge and New York, p 996

Knutson TR, Manabe S (1995) Time-mean response over the tropical Pacific to increased CO_2 in a coupled ocean-atmosphere model. J Clim 8:2181–2199

Knutson TR, Manabe S et al (2010) Tropical cyclones and climate change. Nat Geosci 3(3):157–163

Li T, Kwon M, Zhao M, Kug J, Luo J, Yu W (2010) Global warming shifts Pacific tropical cyclone location. Geophys Res Lett 37:L2I404. doi:10.1029/2010GL045124

Li T, Zhang L, Murakami H (2015) Strengthening of the Walker circulation under global warming in an aqua-planet general circulation model simulation. Atmos. Sci Adv. doi:10.1007/s00376-015-5033-7

Luo JJ, Sasaki W, Masumoto Y (2012) Indian Ocean warming modulates Pacific climate change. Proc Natl Acad Sci 109:18701–18706

Manabe S, Bryan K, Spelman MJ (1990) Transient response of a global ocean-atmosphere model to a doubling of atmospheric carbon dioxide. J Phys Oceanogr 20(5):722–749

Manabe S, Stouffer RJ, Spelman MJ, Bryan K (1991) Transient responses of a coupled ocean-atmosphere model to gradual changes of atmospheric CO_2. Part I. Annual mean response. J Clim 4(8):785–818

McGregor S, Timmermann A, Stuecker MF et al (2014) Recent Walker circulation strengthening and Pacific cooling amplified by Atlantic warming. Nat Clim Chang 4:888–892

Murakami H, Wang B, Kitoh A (2011) Future change of western North Pacific typhoons: projections by a 20-km-mesh global atmospheric model. J Clim 24:1154–1169

Murakami H, Wang B, Kitoh A, Mizuta R, Shindo E (2012) Future changes in tropical cyclone activity projected by multi-physics and multi-SST ensemble experiments using the 60-km-mesh MRI-AGCM. Clim Dyn 39(9–10):2569–2584

Roeckner E et al (1996) The atmospheric general circulation model ECHAM-4: model description and simulation of present-day climate. Max Planck Institute Rep. 218:90

Sandeep S, Stordal F, Sardeshmukh PD, Compo GP (2014) Pacific Walker circulation variability in coupled and uncoupled climate models. Clim Dyn 43(1–2):103–117

Schneider T, O`Gorman PA, Levine XJ (2010) Water vapor and the dynamics of climate changes. Rev Geophys 48:302–323

Trenberth KE, Fasullo JT, Branstator G, Phillips AS (2014) Seasonal aspects of the recent pause in surface warming. Nat Climate Change. doi:10.1038/NCLIMATE2341

Vecchi GA, Soden BJ (2007) Global warming and the weakening of the tropical circulation. J Clim 20:4316–4340

Vecchi GA, Soden BJ, Wittenberg AT, Held IM, Leetmaa A, Harrison MJ (2006) Weakening of tropical Pacific atmospheric circulation due to anthropogenic forcing. Nature 441:73–76

Vecchi GA, Clement A, Soden BJ (2008) Examining the Tropical Pacific's response to global warming. EOS 89:81–83

Wallace JM, Gutzler DS (1981) Teleconnections in the geopotential height field during the Northern Hemisphere winter. Mon Weather Rev 109(4):784–812

Wang B, Wu R, Fu X (2000) Pacific-East Asian teleconnection: how does ENSO affect East Asian climate. J Clim 13:1517–1536

Wang B, Xiang B, Lee JY (2013) Subtropical high predictability establishes a promising way for monsoon and tropical storm predictions. Proc Natl Acad Sci 110(8):2718–2722

Xie SP, Deser C, Vecchi GA, Ma J, Teng H, Wittenberg AT (2010) Global warming pattern formation: sea surface temperature and rainfall. J Clim 23:966–986

Zhang L (2016) The roles of external forcing and natural variability in global warming hiatuses. Clim Dyn. doi:10.1007/s00382-016-3018-6

Zhang L, Li T (2014) A simple analytical model for understanding the formation of sea surface temperature patterns under global warming. J Climate 27(22):8413–8421

Zhao M, Held IM (2010) An analysis of the effect of global warming on the intensity of Atlantic Hurricanes using a GCM with statistical refinement. J Climate 23:6382–6393

Zhao M, Held IM (2012) TC-permitting GCM simulations of Hurricane frequency response to sea surface temperature anomalies projected for the Late 21st century. J Climate 25:2995–3009